THE JOURNAL OF PHYSICAL CHEMISTRY Letters

Letter

pubs.acs.org/JPCL

Competition Between Extinction and Enhancement in Surface-Enhanced Raman Spectroscopy

Thomas van Dijk,[†] Sean T. Sivapalan,[‡] Brent M. DeVetter,[¶] Timothy K. Yang,[§] Matthew V. Schulmerich,[†,∥] Catherine J. Murphy,[‡,§] Rohit Bhargava,[†,∥,⊥] and P. Scott Carney*[,†,¶]

[†]Beckman Institute for Advanced Science and Technology, [‡]Department of Materials Science and Engineering, [¶]Department of Electrical and Computer Engineering, [§]Department of Chemistry, [∥]Department of Bioengineering, and [⊥]Department of Mechanical Science and Engineering, Chemical and Biomolecular Engineering and University of Illinois Cancer Center, University of Illinois at Urbana−Champaign, Urbana, Illinois 61801, United States

ABSTRACT: Conjugated metallic nanoparticles are a promising means to achieve ultrasensitive and multiplexed sensing in intact three-dimensional samples, especially for biological applications, via surface-enhanced Raman scattering (SERS). We show that enhancement and extinction are linked and compete in a collection of metallic nanoparticles. Counterintuitively, the Raman signal vanishes when nanoparticles are excited at their plasmon resonance, while increasing nanoparticle concentrations at off-resonance excitation sometimes leads to decreased signal. We develop an effective medium theory that explains both phenomena. Optimal choices of excitation wavelength, individual particle enhancement factor, and concentrations are indicated. The same processes that give rise to enhancement also lead to increased extinction of both the illumination and the Raman-scattered light. Nanoparticles attenuate the incident field (blue) and at the same time provide local enhancement for SERS. Likewise, the radiation of the Raman-scattered field (green) is enhanced by the nearby sphere but extinguished by the rest of the spheres in the suspension upon propagation.

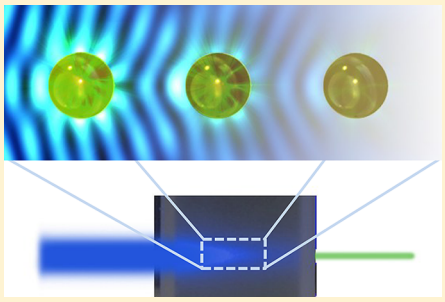

SECTION: Physical Processes in Nanomaterials and Nanostructures

Several methods for using surface-enhanced Raman scattering (SERS)[1] have emerged for biomedical applications, ultrasensitive sensing, and multiplexed analyses. In particular, nanoparticles have been the focus of recent efforts toward in vitro and in vivo molecular sensing.[2−5] Nanoparticles can dramatically increase the electric field intensity near and at their surface, providing useful SERS-based probes,[6] especially for deep tissue imaging at varying concentrations.[7] Typically, a nanostructured particle is bioconjugated and employed in the same manner as conventional fluorescent probes are used for molecular imaging. SERS probes are postulated to offer bright and stable signals and extensive multiplexing,[8] while it has been assumed that experimental best practice parallels that of fluorescent probes, that is, that one should excite at the strongest resonance and use a high concentration. In fact, it has recently been recognized even in single-particle enhancement of fluorescence that peak signals are observed to be red-shifted from the plasmon reference.[9] Thus far, the design of nanoparticle-based SERS experiments has focused on maximizing the local electromagnetic field enhancement in or around an individual particle.[10,11] This strategy fails to take into account the physics of propagation in the bulk medium where the same processes that give rise to enhancement also lead to increased extinction of both the illumination and the Raman-scattered light. Particles provide enhanced fields for Raman scattering, and the same particles form an effective medium with corresponding absorption. The importance of absorption of the Raman-scattered light is recognized in ref 12. However, they do not describe the necessary link and competition between the enhancement and the extinction. For example, it is commonly known to experimentalists that gold nanospheres exhibit a plasmon resonance at 520 nm and should produce a large local field enhancement when illuminated at 532 nm; yet, no appreciable Raman signal is observed upon 532 nm excitation commonly ascribed to interband transitions in gold.[13] Away from the plasmon resonance frequency maximum, the Raman signal is again observed and actually increases as the excitation wavelength becomes longer.

In this Letter, we address the issue of extinction by a suspension of nanoparticles in SERS experiments through an effective medium approach. It is shown that extinction and enhancement are tied to each other and compete in such a way that peak signals are acquired off-resonance and that, at any wavelength, an optimal particle concentration exists to maximize the Raman signal. We provide verification of the model with experiments in which the particle concentration is varied.

Propagation of light in a dilute suspension of identical particles is well-approximated by propagation through a

Received: March 6, 2013
Accepted: March 22, 2013
Published: March 22, 2013

homogeneous medium with an effective refractive index $\tilde{m}$, given by[14]

$$\tilde{m} = m\left[1 + \mathrm{i}\frac{2\pi\rho}{k^3}S(0)\right] \tag{1}$$

where m is the refractive index of the medium in which the particles are embedded, $k = \omega/c$ is the wavenumber in the medium, ρ is the number of particles per unit volume, and $S(0)$ is the scattering amplitude in the forward direction.[14] The absorption coefficient in a medium with a complex refractive index is $\alpha = 2k\,\mathrm{Im}\,\tilde{m}$. For a suspension with small identical particles, the absorption coefficient is given by $\alpha = m4\pi\rho k^{-2}\,\mathrm{Re}[S(0)] = \rho m C_{\mathrm{ext}}$, where C_{ext} is the extinction cross section of a single particle in the suspension, proportional to the real part of the forward-scattering amplitude. The attenuation of a well-collimated beam propagating through the effective medium is described by Beer's law,[15] $I(h) = I(0)\mathrm{e}^{-hm\rho C_{\mathrm{ext}}}$, where I is the intensity and h is the propagation distance. The extinction cross section, rather than the absorption cross section, is used to account also for scattering out of the collection and detection optical train or subsequent absorption. Hence, for systems of large particles, where the scattering is mostly in the forward direction, or for high-NA systems, this model may fail or require correction for contribution to the detection by the scattered field. In the system considered here, the particles are small compared to the wavelength, and the optical system is low-NA.[16]

The extinction cross section, C_{ext}, for a small metallic sphere with radius a, to terms of order $(ka)^4$, is given by[14]

$$C_{\mathrm{ext}} = 4k\pi a^3\,\mathrm{Im}\left\{\frac{p^2-1}{p^2+2}\left[1 + \frac{(ka)^2}{15}\left(\frac{p^2-1}{p^2+2}\right)\times\frac{p^4+27p^2+38}{2p^2+3}\right]\right\} + \frac{8}{3}(ka)^4 \times \pi a^2\,\mathrm{Re}\left[\left(\frac{p^2-1}{p^2+2}\right)^2\right] \tag{2}$$

where $p = m_s/m$ is the ratio of the refractive index of the material of the spheres, m_s, to that of the refractive index of the medium, m, which both depend on the wavenumber. For dilute suspensions, the change in the real part of the refractive index of the effective medium from the background is negligible. The extinction from gold spheres in a suspension is shown in Figure 1, where the extinction peaks near the Fröhlich frequency ($\lambda_f \approx$ 520 nm); for this calculation the optical constants obtained by Johnson and Christy for gold have been used.[17]

The Raman signal, which we denote as R, from a single, isolated nanoparticle depends on the incident field amplitude, E_0, the number of Raman-active molecules, N, the local field enhancement, $f(\mathbf{r},\omega)$, and the spatial distribution of those molecules. This last point we address through a probability density, which in general will also depend on the number of molecules present, $p(\mathbf{r}, N)$. Though not explicitly noted, the local enhancement factor is also dependent on the orientation of the incident electric field vector. The number of molecules attached to the nanoparticle may itself be random and given by the probability of finding N molecules attached to the particle P_N. A single molecule at $\mathbf{r}$ is excited by a field with amplitude $E_0 f(\mathbf{r},\omega_0)$, producing a secondary source proportional to the

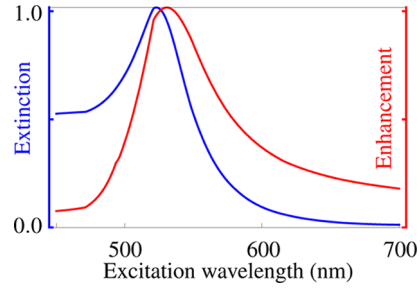

Figure 1. (blue) The normalized extinction cross section C_{ext} from eq 2. Extinction by gold spheres of 5 nm radius in aqueous suspension as a function of the wavelength of the incident light. (red) The normalized Raman enhancement, $G(\lambda)$ from eq 4, versus the excitation wavelength for gold spheres of radius much smaller than the wavelength evaluated for a Raman shift of 0 nm.

Raman susceptibility χ, which implicitly depends on ω_0, and ω. The field reradiated at the Raman-shifted frequency ω is enhanced by the particle as well, so that, by reciprocity, the reradiated field is proportional to $\chi E_0 f(\mathbf{r},\omega_0) f(\mathbf{r},\omega)$. We assume that the Raman signal from each reporter molecule is statistically independent; therefore, the intensities add. The ensemble-averaged Raman signal for a single nanoparticle is thus given by

$$R = |\chi|^2 \sum_{N=1}^{\infty} NP_N \int \mathrm{d}^3 r\, |E_0 f(\mathbf{r},\omega_0) f(\mathbf{r},\omega)|^2 p(\mathbf{r},N) = \langle N\rangle G R^{(0)} \tag{3}$$

where $R^{(0)}$ is the Raman signal from one molecule absent the particle and G is the Raman enhancement factor and generally depends on $p(\mathbf{r},N)$ and P_N. For systems in which the particle placement is independent of the number of particles, the sum and the integral may be carried out independently, the sum yielding the average number of molecules $\langle N\rangle$, and the integral resulting in a G independent of the number of molecules.

The enhancement factor for a small sphere of radius a ($a \ll \lambda$) with a uniform probability of molecule placement over the surface of the sphere can be calculated in closed form[18]

$$G(\omega,\omega_0) = |[1 + 2g(\omega_0)][1 + 2g(\omega)]|^2 \tag{4}$$

where $g = (p^2-1)/(p^2+2)$, ω_0 is the frequency of the incident field, and ω is the frequency of the Raman-scattered field.

The enhancement calculated by eq 4 is shown in Figure 1 alongside the extinction using the optical constants obtained by Johnson and Christy.[17] It is clear that enhancement and extinction are closely linked and that when the enhancement is strong, the correspondingly strong extinction must be taken into account. The light falling on a single particle is attenuated by propagation through the suspension and arrives with amplitude attenuated by the factor $\exp[-\int_0^z \mathrm{d}z'\,\rho(z')\,mC_{\mathrm{ext}}(\omega_0)/2]$. The local Raman signal is then $\langle N\rangle\, R^{(0)} G\rho(z)\,\exp[-\int_0^z \mathrm{d}z'\,\rho(z')mC_{\mathrm{ext}}(\omega_0)]$. In transmission mode, this signal must then propagate out through the medium to $z = h$, and the intensity is attenuated by a factor of $\exp[-\int_z^h \mathrm{d}z'\,\rho(z')\,mC_{\mathrm{ext}}(\omega)]$. The total signal is a sum over the signal from all particles, so that

dx.doi.org/10.1021/jz4005043 | J. Phys. Chem. Lett. 2013, 4, 1193−1196

$$R = \langle N\rangle A R^{(0)} G \int_0^h dz\ \rho(z)\exp\left[-\int_0^z dz'\ \rho(z')\right.$$
$$\left.\times\ mC_{ext}(\omega_0)\right]\exp\left[-\int_z^h dz'\ \rho(z')mC_{ext}(\omega)\right] \quad (5)$$

where A is the integral over the transverse beam profile normalized to the peak value, the effective transverse area of the beam. When the concentration $\rho(z)$ does not depend on z, the integrals can be computed in closed form with the result

$$R = \langle N\rangle A R^{(0)} G \frac{e^{-mC_{ext}(\omega_0)h\rho} - e^{-mC_{ext}(\omega)h\rho}}{mC_{ext}(\omega) - mC_{ext}(\omega_0)} \quad (6)$$

From this expression, it is seen that there are two competing processes that determine the size of the Raman signal, the enhancement, G, and the extinction that results in a exponential decay of the signal. The same processes that increase the enhancement also increase the extinction. The attenuation due to extinction depends not only on the frequency but also on the concentration of the nanospheres. This is illustrated in Figure 2a, where it is shown that for increasing concentration, the peak

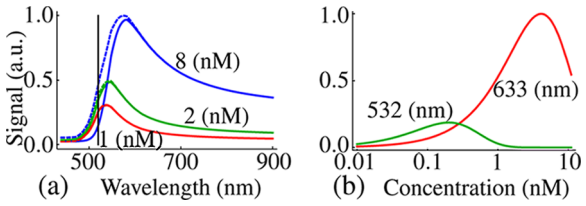

Figure 2. (a) Solid lines: Predicted signal in transmission mode versus the wavelength of the incident light. Dashed lines: Predicted signal in reflection mode versus the wavelength of the incident light. Both transmission and reflection signals are with three different concentrations of the nanospheres that have a radius 6 nm; the sample thickness h is 2 cm. The vertical black line indicates the location of the surface plasmon resonance. (b) Predicted signal in transmission mode versus the concentration for two different incident wavelengths; the radius of the spheres is 15 nm.

of the signal is shifted farther away from the resonant wavelength. This result explains the absence of Raman signal at the plasmon resonance where extinction is so strong that no signal is observed.

In reflection mode, there is always a contribution from the front layer of the sample that is not attenuated, and therefore, the expression for the Raman signal is slightly altered

$$R = \langle N\rangle A R^{(0)} G \frac{1 - e^{-hm\rho[C_{ext}(\omega)+C_{ext}(\omega_0)]}}{mC_{ext}(\omega) + mC_{ext}(\omega_0)} \quad (7)$$

The Raman signal in reflection mode for three different concentrations of the nanospheres is shown in Figure 2a as the dashed lines. In the reflection mode, there is a slightly higher signal to the blue side of the resonance compared to the signal in transmission mode.

The Raman signal in transmission mode is depicted in Figure 2b for two commonly used wavelengths evaluated for a Raman band at 1076 cm^{-1}. For λ = 532 nm, the excitation wavelength closest to the plasmon resonance, the signal is very small. A higher signal is found farther away from resonance with the peak shifted to the red. For relatively low concentrations, the biggest signal is obtained with a wavelength of 632 nm. Only for concentrations smaller than 0.1 nM is the signal bigger for the excitation wavelength closest to resonance, as shown in Figure 2b. It is seen that there is a concentration that maximizes the signal. This optimal concentration, ρ_{opt}, can be found by differentiating eq 6 and equating it to zero, giving the following expression

$$\rho_{opt} = \frac{\ln[C_{ext}(\omega)/C_{ext}(\omega_0)]}{hm[C_{ext}(\omega) - C_{ext}(\omega_0)]} \quad (8)$$

When the extinction cross section, $C_{ext}(\omega)$, equals, or is very close to, $C_{ext}(\omega_0)$, the optimal concentration becomes $\rho_{opt} = 1/[hmC_{ext}(\omega_0)]$. The strong nonlinearity with concentration that these competing phenomena impose on the recorded signal is also a caution in the development of practical assays and must be taken into account to correctly quantify results across samples. Hence, this physics-based analysis enables quantitative molecular imaging for SERS-based microscopy.

The model presented in this paper is validated by measuring the SERS signal of 4,4′-dipyridyl Raman reporter molecules attached to gold nanospheres. Spectra were acquired from the nanoparticles in suspension using a high-resolution Raman spectrometer (LabRAM, Horiba) with a 90 s acquisition time. The Raman shift from 200 to 1800 cm^{-1} was collected at 10 cm^{-1} resolution with 10 mW laser power at the sample. Transmission Raman measurements were collected by focusing laser light through a 1 cm cuvette with a 50 mm focal length lens and collected with a 100 mm focal length lens to collimate the transmitted light and direct it to the spectrograph.

The integrated SERS signal under three different bands (476, 1076, and 1600 cm^{-1}) is compared for different concentrations of the gold spheres when excited at 632 nm. The SERS spectra from 4,4′-dipyridyl for increasing concentrations is illustrated in Figure 3a. The three boxes indicate the Raman bands for which

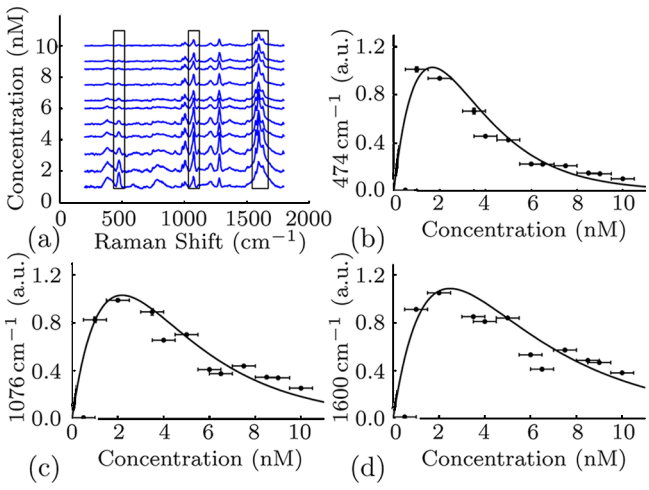

Figure 3. (a) SERS spectra of 4,4′-dipyridyl attached to gold nanospheres with a radius of 15 nm at an excitation wavelength of 633 nm at different nanoparticle concentrations. Measured Raman signals (points) agree with the theoretical prediction (solid line) for a Raman shift of (b) 474, (c) 1076, and (d) 1600 cm^{-1}.

the signal is investigated as a function of concentration. The signal is obtained by integrating the Raman band of interest over the width of the box, as shown in Figure 3.

As predicted, increasing the concentration of nanoparticles in an attempt to increase the signal leads to signal attenuation beyond an optimal concentration. The measurements are in good agreement with the model. Our results suggest that strategies to increase Raman signals using nanoparticles should

dx.doi.org/10.1021/jz4005043 | J. Phys. Chem. Lett. 2013, 4, 1193−1196

not focus on achieving greater local enhancement but instead might strive for designs that maximize total signal by separating the single-particle enhancement and absorption peaks or otherwise tailoring the shape of the enhancement and absorption curves to maximize the gap between absorption and enhancement at frequencies away from resonance. A move toward using thin samples with large areas of collection is also suggested. We see that the signal is increased by moving away from resonance and, in some cases, by lowering the concentration of particles. While we focused on nanospheres, our results apply broadly to particle-based Raman enhancement with nonspherical particles as well.

EXPERIMENTAL METHODS

Gold nanospheres of 15 nm radius were synthesized by the boiling citrate method.[19,20] For stability against aggregation, 100 mg of bis(*p*-sulfonatophenyl)phenylphosphine dihydrate dipotassium salt (BSPP) was added to 100 mL of as-synthesized nanoparticles.[21,22] The mixture was left to stir overnight (12−16 h), and excess reagents were removed by two centrifugation cycles (3000 RCF, 20 min). For 4,4′-dipyridyl complexation, 1 mL of 10 mM 4,4′-dipyridyl in water was added to 9 mL of BSPP-stabilized gold nanoparticles and left to complex overnight.[23] Excess reagents were removed by two centrifugation cycles (3000 RCF for 20 min). For final purification, we dialyzed the solutions in Thermo Scienfific G2 Slide-A-Lyzer G2 cassettes against 4 L of Barnstead E-Pure (18 MΩ cm) water for 48 h.

AUTHOR INFORMATION

Corresponding Author

*E-mail: carney@uiuc.edu.

Notes

The authors declare no competing financial interest.

ACKNOWLEDGMENTS

The work was supported in part by the Beckman Fellows program. S.T.S. and B.M.D. acknowledge support from the University of Illinois at Urbana−Champaign from the NIH National Cancer Institute Alliance for Nanotechnology in Cancer "Midwest Cancer Nanotechnology Training Center" Grant R25CA154015A. M.V.S. acknowledges support through the Congressionally Directed Medical Research Program Postdoctoral Fellowship BC101112. We also acknowledge support from a Beckman Institute seed grant, AFOSR Grant No. FA9550-09-1-0246, and NSF Grants CHE-1011980 and CHE-0957849.

REFERENCES

(1) Schatz, G. C.; Van Duyne, R. P. *Handbook of Vibrational Spectroscopy*; John Wiley & Sons: Chichester, U.K., 2002; Vol. *1*, pp 759−774.

(2) Lyandres, O.; Yuen, J. M.; Shah, N. C.; van Duyne, R. P.; Walsh, J. T.; Glucksberg, M. R. Progress Toward an In Vivo Surface-Enhanced Raman Spectroscopy Glucose Sensor. *Diabetes Technol. Ther.* **2008**, *10*, 257−265.

(3) Qian, X.; Peng, X.-H.; Ansari, D. O.; Yin-Goen, Q.; Chen, G. Z.; Shin, D. M.; Yang, L.; Young, A. N.; Wang, M. D.; Nie, S. In Vivo Tumor Targeting and Spectroscopic Detection with Surface-Enhanced Raman Nanoparticle Tags. *Nat. Biotechnol.* **2008**, *26*, 83−90.

(4) von Maltzahn, G.; Centrone, A.; Park, J.-H.; Ramanathan, R.; Sailor, M. J.; Hatton, T. A.; Bhatia, S. N. SERS-Coded Gold Nanorods as a Multifunctional Platform for Densely Multiplexed Near-Infrared Imaging and Photothermal Heating. *Adv. Mater.* **2009**, *21*, 3175−3180.

(5) Frontiera, R. R.; Henry, A.-I.; Gruenke, N. L.; Van Duyne, R. P. Surface-Enhanced Femtosecond Stimulated Raman Spectroscopy. *J. Phys. Chem. Lett.* **2011**, *2*, 1199−1203.

(6) Larmour, I. A.; Argueta, E. A.; Faulds, K.; Graham, D. Design Consideration for Surface-Enhanced (Resonance) Raman Scattering Nanotag Cores. *J. Phys. Chem. C* **2012**, *116*, 2677−2682.

(7) Stone, N.; Faulds, K.; Graham, D.; Matousek, P. Prospects of Deep Raman Spectroscopy for Noninvasive Detection of Conjugated Surface Enhanced Resonance Raman Scattering Nanoparticles Buried within 25 mm of Mammalian Tissue. *Anal. Chem.* **2010**, *82*, 3969−3973.

(8) Cao, Y. C.; Jin, R. C.; Nam, J. M.; Thaxton, C. S.; Mirkin, C. A. Raman Dye-Labeled Nanoparticle Probes for Proteins. *J. Am. Chem. Soc.* **2003**, *125*, 14676−14677.

(9) Bharadwaj, P.; Novotny, L. Spectral Dependence of Single Molecule Fluorescence Enhancement. *Opt. Express* **2007**, *21*, 14266−14274.

(10) Talley, C. E.; Jackson, J. B.; Oubre, C.; Grady, N. K.; Hollars, C. W.; Lane, S. M.; Huser, T. R.; Nordlander, P.; Halas, N. J. Surface-Enhanced Raman Scattering from Individual Au Nanoparticles and Nanoparticle Dimer Substrates. *Nano Lett.* **2005**, *5*, 1569−1574.

(11) Kodali, A. K.; Llora, X.; Bhargava, R. Optimally Designed Nanolayered Metal−Dielectric Particles as Probes for Massively Multiplexed and Ultrasensitive Molecular Assays. *Proc. Natl. Acad. Sci. U.S.A.* **2010**, *107*, 13620−13625.

(12) Jackson, J. B.; Westcott, S. L.; Hirsch, L. R.; West, J. L.; Halas, N. J. Controlling the Surface Enhanced Raman Effect via the Nanoshell Geometry. *Appl. Phys. Lett.* **2003**, *82*, 257−259.

(13) Alvarez-Puebla, R. A. Effects of the Excitation Wavelength on the SERS Spectrum. *J. Phys. Chem. Lett.* **2012**, *3*, 857−866.

(14) Bohren, C. F.; Huffman, D. R. *Absorption and Scattering of Light by Small Particles*; Jon Wiley and Sons: New York, 1983.

(15) van de Hulst, H. C. *Light Scattering by Small Particles*; Dover Publications: Mineola, NY, 1982.

(16) Bohren, C. F. Applicability of Effective-Medium Theories to Problems of Scattering and Absorption by Nonhomogeneous Atmospheric Particles. *J. Atmos. Sci.* **1986**, *43*, 468−475.

(17) Johnson, P. B.; Christy, R. W. Optical-Constants of Noble-Metals. *Phys. Rev. B* **1972**, *6*, 4370−4379.

(18) Kerker, M.; Wang, D. S.; Chew, H. Surface Enhanced Raman-Scattering (SERS) by Molecules Absorbed at Spherical-Particles: Errata. *Appl. Opt.* **1980**, *19*, 4159−4174.

(19) Ji, X.; Song, X.; Li, J.; Bai, Y.; Yang, W.; Peng, X. Size Control of Gold Nanocrystals in Citrate Reduction: The Third Role of Citrate. *J. Am. Chem. Soc.* **2007**, *129*, 13939−13948.

(20) Kimling, J.; Maier, M.; Okenve, B.; Kotaidis, V.; Ballot, H.; Plech, A. Turkevich Method for Gold Nanoparticle Synthesis Revisited. *J. Phys. Chem. B* **2006**, *110*, 15700−15707.

(21) Loweth, C. J.; Caldwell, W. B.; Peng, X. G.; Alivisatos, A. P.; Schultz, P. G. DNA-Based Assembly of Gold Nanocrystals. *Angew. Chem., Int. Ed.* **1999**, *38*, 1808−1812.

(22) Schmid, G.; Lehnert, A. The Complexation of Gold Colloids. *Angew. Chem., Int. Ed. Engl.* **1989**, *28*, 780−781.

(23) Lim, D. K.; Jeon, K. S.; Hwang, J. H.; Kim, H.; Kwon, S.; Suh, Y. D.; Nam, J. M. Highly Uniform and Reproducible Surface-Enhanced Raman Scattering from DNA-Tailorable Nanoparticles with 1-nm Interior Gap. *Nat. Nanotechnol.* **2011**, *6*, 452−460.